Available online at www.sciencedirect.com
SCIENCE DIRECT®
ELSEVIER
International Journal of Multiphase Flow 29 (2003) 1817–1831
International Journal of Multiphase Flow
www.elsevier.com/locate/ijmulflow

Self-lubricated transport of aqueous foams in horizontal conduits

M.I. Briceño [a], D.D. Joseph [b,*]

[a] *Laboratorio FIRP, University of Los Andes, Mérida, 5101 Venezuela*
[b] *Department of Aerospace Engineering and Mechanics, University of Minnesota, AEM 107 Aderman Hall, 110 Union Street, 121 Akerman Hall, Minneapolis 55455, USA*

Received 15 May 2003; received in revised form 1 October 2003

Abstract

The flow characteristics of aqueous foams were studied in a thin flow channel and a round pipe instrumented for pressure gradient and flow rate measurements. The quality of the foam was varied by controlling the volumetric flow rate of liquid and gas, and different flow types were identified and charted. Uniform foams move as a rigid body lubricated by water generated by breaking foam at the wall. A lubrication model leading to a formula for the thickness of the lubricating layer is presented. The formula predicts a layer thickness of 6–8 μm in the channel and 10–12 μm in the pipe. The thickness depends weakly on foam quality. An overall correlation for the friction factor as a function of Reynolds number which applies to both channel and pipe is derived. This correlation is consistent with a model in which a rigid core of foam is lubricated by laminar flow of a water layer in the range of measured thickness.

Keywords: Foam; Lubrication; Flow pattern; Foam quality; Lubrication foam flow in pipes

1. Introduction

Foams are encountered in many industrial applications; they are used as cleaning fluids, fire mitigators and in froth flotation in the paper and metallurgy industry. Many cosmetics and foods are foams. Applications for flowing foams are also abundant. In the oil industry, foams are used in under-balanced drilling, for reservoir clean-up and for enhanced oil recovery in porous sand.

* Corresponding author. Tel.: +1-612-625-0309; fax: +1-612-626-1558.
E-mail address: joseph@aem.umn.edu (D.D. Joseph).

0301-9322/$ - see front matter
doi:10.1016/j.ijmultiphaseflow.2003.10.001

For these applications, the flow characteristics depend on the flow types which surprisingly have not been charted.

In this paper, we study aqueous foams flowing through a horizontal slit channel and a round pipe. For these configurations we chart the flow types and analyze the flow resistance. Special attention is given to the flow properties of uniform foams. It is found that the flow of such foams is *not* controlled by foam rheology. These uniform flows *self-lubricate* as in the pipeline transport of bitumen (Joseph et al., 1999), but the self-lubrication is driven by different mechanisms in the two cases. The self-lubricated foam moves forward as a rigid body lubricated by water. The water layer is small and not uniform; it is formed by the breaking and the healing of the foam at the conduit walls. The main principle underway is that *it is easier to break than to deform the foam.*

The conditions under which foams self-lubricate, as in the experiments reported here, are not yet known.

2. Literature

The description of flowing foams found in the literature is based implicitly on the idea that the flow behavior of foams can be described by models used for non-Newtonian fluids such as power law fluids (Deshpande and Barigou, 2000; Deshpande and Barigou, 2001a,b; Valkó and Economides, 1992; Enzerdofer et al., 1995; Gardiner et al., 1998; Heller and Kuntamukkula, 1987), as power law fluids with a yield stress (see, for example, Khan et al., 1988; Khan, 1987; Khan and Armstrong, 1986; Calvert and Nezhati, 1986) or as power law fluids with wall slip (Rojas et al., 2001; Bekkour, 1999; Gardiner et al., 1998; Enzerdofer et al., 1995) using the classical method of Mooney (1931) and Oldroy–Jastrzebski (1967) for correction of slip.

For the case of wet foams, the apparent slip is produced by a thin layer of liquid that according to Tisnè et al. (2003), who actually measured film thickness in a horizontal square duct, is produced by the migration of bubbles away from the solid boundaries.

As mentioned above, foam flow types have not been charted before although previous works carried out in a square horizontal channel (Tisnè et al., 2003; Blondin and Doubliez, 2002) and in a horizontal pipe (Calvert, 1990) have identified stratified flow (a partially sheared or unsheared layer of foam on top of a sheared layer of liquid) for wet aqueous foams. Prior work relevant to self-lubrication of foams was carried out in our Minnesota laboratory and is reported in the Master's dissertation of Smieja (2000). He worked only with a slit channel but produced data for vertical as well as horizontal channels. The present work follows and greatly extends this prior work.

Measurements of foam rheology are appropriate for conditions under which the flowing foam deforms. The flow of foams requires less foam deformation when the foam slips at the wall. Here, we are putting forward the idea that slip is induced by breaking foam at the conduit walls. If it is much easier to break than to deform the foam, slip will be complete and flow will self-lubricate with foam flowing in a rigid core lubricated by water.

3. Experimental setup

The foam was prepared by mixing a surfactant solution with compressed air in a foam generator. The surfactant solution consisted of two components, 0.6% w/w of an anionic surfactant,

sodium dodecyl sulphate, made by Aldrich, 98% pure, and 1% w/w of a co-surfactant, 1-butanol, made by Fisher. These components were diluted in 22.7 l of de-ionized water. The foam produced by means of these surface-active components was sufficiently stable under flow and could persist for a few minutes in static conditions.

The experimental setup is shown in Fig. 1. The surfactant solution was contained in a large plastic vessel where the foam, which would take much of the vessel volume, would break to recover the solution. The latter was pumped through the test section by means of a Dayton split phase pump model 6K160C. The liquid flow was regulated by means of a vane valve placed at the pump discharge and also by regulating the recirculation flow to the vessel. The volumetric flow rate was measured using a Gilmont rotameter, model #15, previously calibrated.

A pressure regulator that would provide air at 18–22 psig first handled compressed air from main supply. Air volumetric flow rate was measured by means of an Omega rotameter, model FL-3804G; this model has a fine regulating flow valve. The manufacturer calibration curve was used to convert meter readings to l/min units. Monitoring compressed air temperature and pressure at the outlet of the air meter by means of an absolute pressure manometer, allowed for corrections for temperature and atmospheric pressure deviations since calibration curve was obtained at 294 K (70 °F) and 1 atm.

Air and surfactant solution were mixed at a tee junction and the mixture was refined in a foam generator consisting of a metal porous plate (pore size 125 μm) followed by a bed of 3 mm glass beads. The foam would then enter the test section that was a 5/8 in. inner diameter pipe or a closed channel or slit, 1 in. tall and 1/4 in. wide; both conduits were made of transparent Plexiglas and were 1.2 m long. The circular pipe was equipped with four equally distanced (25 cm) pressure transducers, made by Omega; the first two up-stream transducers (P_1 and P_2, see Fig. 1), were model PX800-002GV, 2.5 psi maximum pressure and the last two were (P_3 and P_4) model PX800-001GV, 1 psi maximum pressure. Each transducer was calibrated against an U-tube manometer, made by Dwyer, filled with de-ionized water. Deviations of transducers readings respect to the manometer's was less than 1%.

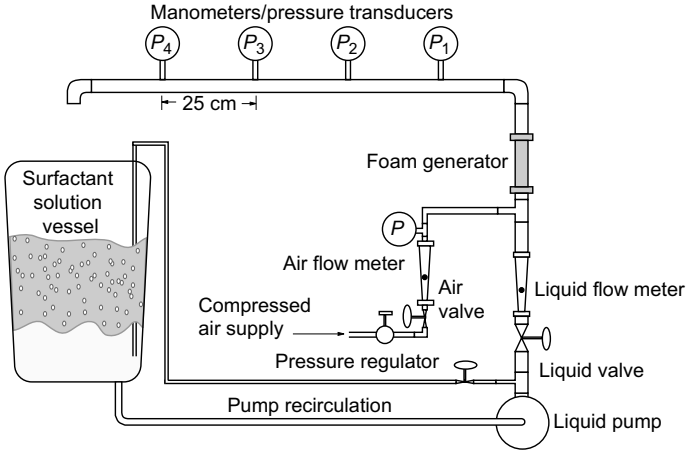

Fig. 1. Schematics of experimental setup (not in scale).

Pressure readings in the closed channel were carried about using two foam trapping taps consisting of short plexiglass cylinders flush mounted on the channel vertical wall and connected to channel interior by means of a small perforation. Previous to a flow test, the bottom of each taps was filled with de-ionized water; during a test, the foam would tend to enter into the tap, but would break upon contact with the water well. Each tap was connected to U-tube manometers; the first contained de-ionized water and the second isopropyl alcohol. Distance between taps was 75 cm, which is the same distance between the first (P_1) and the last pressure transducers (P_2) in the circular pipe.

Before carrying about the very first experimental run, a more concentrated surfactant solution was allowed to circulate trough the system in order to saturate solid surfaces and avoid later loss of surfactant and alcohol molecules by adsorption during a test. Every experimental run proceeded as follows. The pump would be started and the surfactant solution recirculated for at least 30 min, to ensure solution homogeneity. Then, both air valve and liquid valve would be opened and both flows adjusted to the desired values. Liquid flow rate was checked by collecting samples of foam at the end of the test section, and by measuring the time during which the sample was collected. The sample was weighed in a precision balance (made by SARTORIUS, model E5500 S) and, given the liquid density, the liquid flow rate was readily calculated. It has to be noted that the main contribution to foam mass comes from the water fraction; anyhow, this was verified by weighing a sample of fresh, very high quality foam (98%), waiting for the foam to break completely and weighing the remaining liquid solution. The air mass fraction lost was less than 2% of the total foam mass.

Once the required flow rates were reached and verified, gas pressure as well as conduit pressure profile would be monitored until readings were stable. Less than 5 min were required to reach steady state, though at least 10 min elapsed before registering flow rates, gas pressure and test section pressure profile. The type of flow was also recorded for every run.

A total of 71 data points for the closed channel and 54 for the circular pipe were collected and four different surfactant solution batches were used. Some of the runs were repeated several times in order to evaluate repeatability of pressure measurements. It was found that repeatability was better than 5% (variation coefficient) for the majority of the evaluated data, although some data showed values of up to 20%. Data dispersion is more pronounced for the channel; in occasions, some foam penetrates the trapping taps and does not break fast enough. This condition may produce higher scatter of the data.

The volumetric flow rates of water and gas are designated as Q_L and Q_G, respectively. The foam quality is

$$\Gamma = \frac{Q_G}{Q_G + Q_L}. \tag{1}$$

Foam quality was varied from about 40% to 98%. Pressure at the entrance of the conduit was about 99 ± 3 kPa and pressure drop was always lower than 20 kPa or 0.2 bar.

4. Flow patterns

Flow patterns were observed and recorded for every experimental run after the system had reached steady state. Most of the observations were in the slit channel through the large window

($1'' \times 1/4''$). Flow visualization in the slit channel was very reliable and different patterns could be easily distinguished (see Figs. 2 and 3). Movies of flowing foams showing flow patterns can be seen at http://www.aem.umn.edu/research/lubricated-foam/. Only limited observations were possible for the pipe since wall curvature impedes a clear flow visualization. It is important to note that designated values of quality for frontiers between regions are approximate. Seven flow patterns were observed:

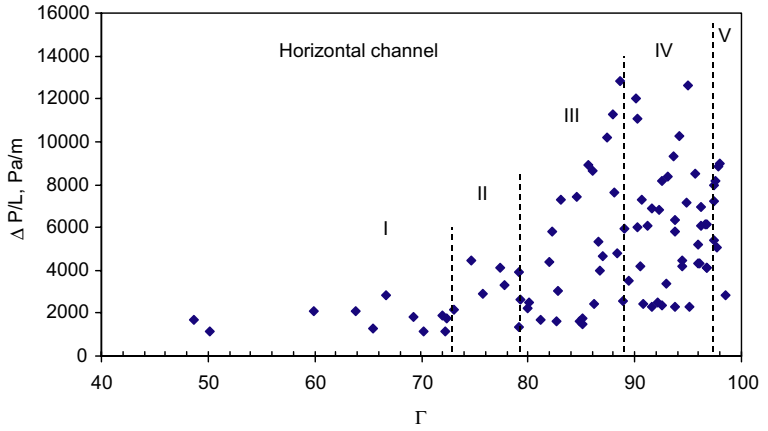

Fig. 2. Pressure gradient as a function of foam quality for the closed horizontal channel, showing some of the patterns observed. *Pattern I*: flow is stratified, a layer of foam flowing in plug flow on top of a thinner layer of liquid. *Pattern II*: liquid layer becomes thinner while limited relative motion between bubbles is observed. *Pattern III*: bottom liquid layer disappears to the naked eye and bubbles churn. *Pattern IV*: Churning vanishes and foam flows in plug flow. *Pattern V*: large air bubble appear and coalesce into large air pockets interspersed by foam slugs.

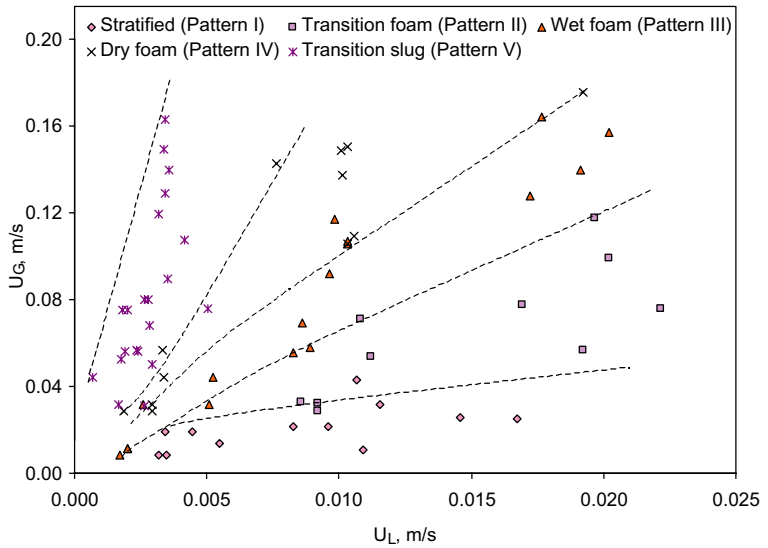

Fig. 3. Flow pattern map of superficial gas velocity U_G vs. superficial liquid velocity U_L.

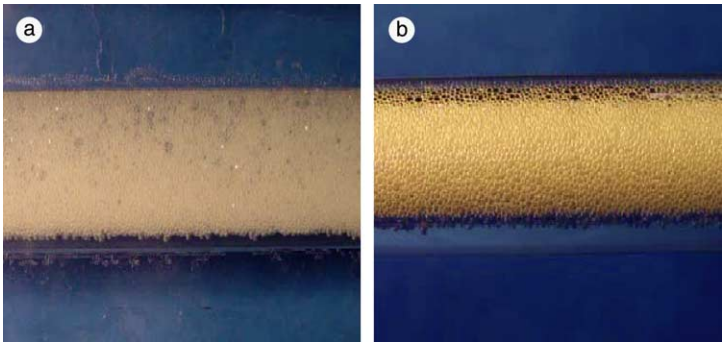

Fig. 4. Flow patterns in a horizontal pipe (a) and channel (b) of low quality foam ($\Gamma < 70\%$). The flow is stratified vertically in two ways: (1) foam above and drained liquid below, (2) stratification in the foam with large bubbles on top.

Pattern I ($\Gamma < 73\%$): The fluid flows forming two distinct layers, one on top of the other. It is very similar to stratified flow although the top layer is relatively dry foam that flows with no apparent relative motion between the bubbles (plug flow); this top layer rides above a liquid film that drains almost instantly at the entrance of the horizontal channel. A similar behavior was also observed for the pipe. There is bubble size segregation, the smaller at the bottom and the largest at the top. Fig. 4 shows two photographs depicting the two-layer motion in the pipe (a) and in the channel (b), for quality below 70%.

Pattern II ($73\% < \Gamma < 79\%$): The bottom liquid films becomes very thin and the top foam bubbles move respect to each other in a very limited fashion; not much churning occurs. Bubbles closer to the liquid film move faster that the bubbles close to the upper wall. There is also bubble size segregation, the smaller at the bottom and the largest at the top.

Pattern III ($79\% < \Gamma < 89\%$): The drainage film vanishes, at least to the naked eye, and a mixed or churn flow occurs while bubble segregation by size disappears. A blunt profile is established in which the maximum velocity is displaced to the bottom of the channel.

Pattern IV ($89\% < \Gamma < 97\%$): This is a plug flow pattern which we have described as self-lubricated foam; air bubbles have the same speed and no shear is observed. Time sequence photographs of a 94% quality foam at a liquid flow rate of 0.1 l/min, taken at time intervals of 6 ms, are shown in Fig. 5. Lines drawn between readily identified bubbles across the channel do not

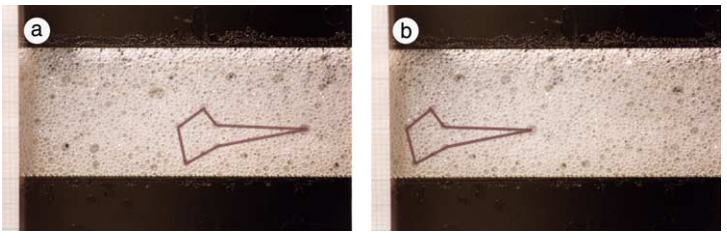

Fig. 5. Time sequence photographs of a flowing foam in the channel, for liquid rate of 0.02 l/min; (a) first photograph; (b) after 6 ms. An irregular figure has been drawn to show that, after 6 ms, the relative position of a selected bubble array has not changed, indicating that foam flows as a rigid plug which slips at the wall and is not sheared internally. Movies of this flow can be found at http://www.aem.umn.edu/research/lubricated-foam/.

stretch or rotate; this shows that the foam is not sheared and is moving forward as a rigid plug. Fig. 6 shows that this high quality foam is much like a wimpy solid (viscoplastic), very similar to shaving or whipped cream. Pattern IV behavior also occurs in round pipes and is documented in the movies on our web site.

Pattern V ($\Gamma > 97\%$): When the foam quality is very large, the uniform dispersion gives way to a nonhomogeneous dispersion in which some gas collects into the large bubbles shown in Fig. 7(b). This nonhomogeneous flow pattern is transitional between uniform and slug flow shown in Fig. 8.

Pattern VI ($\Gamma > 98\%$): As the quality of the foam approaches 99%, gas bubbles coalesce into large gas pockets separated by foam slugs shown in Fig. 8. The slugs are retarded by wall friction; the gas pockets move faster than the foam in an average sense. Typically, foam is retarded more at the bottom because the gas pockets are lighter.

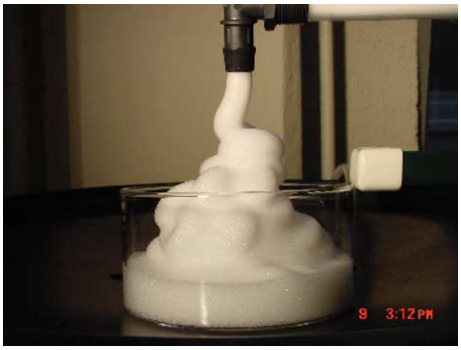

Fig. 6. Photograph of foam exiting the pipe, exhibiting viscoplastic behavior; flow conditions correspond to the plug flow pattern IV shown in Figs. 5 and 7(a).

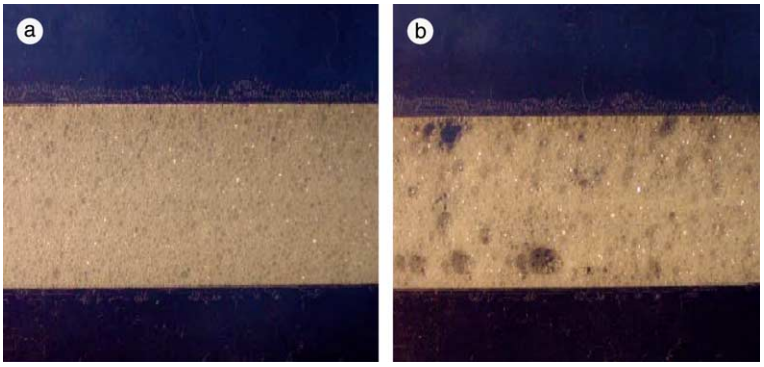

Fig. 7. Flow patterns observed for horizontal flow in channel in (a) pattern IV ($\Gamma \cong 95\%$) where flow is plug type and in (b) pattern V ($\Gamma \cong 97\%$) where flow is still plug like though large bubbles appear as a transition to slug flow. These large bubbles grow much larger if gas flow rate is further increased and eventually coalesce to produce air pockets or slug flow (see Fig. 8).

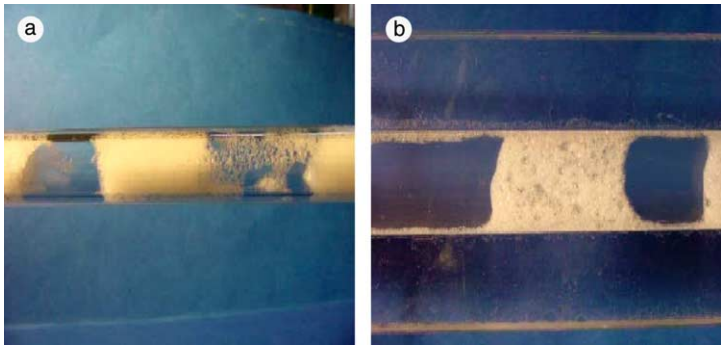

Fig. 8. Slug flow ($\Gamma > 98\%$) in (a) pipe and (b) channel.

Pattern VII ($\Gamma > 99\%$): When the gas flow rate is very high it is not possible to move slugs of foam fast enough and the gas breaks through. The foam covers parts of the wall in bits and pieces but does not span the pipe.

We compared our results with those of Smieja (2000) who did observations in a vertical rather than in a horizontal channel. The main difference is due to the effects of gravity which induces intense mixing and churning in wet foams because large gas bubbles rise much faster than the wet foam. The effects of gravity are much less when the gas is trapped in the cells of a drier and more uniform foam. Flow patterns in horizontal and vertical flow are the same when the quality is above about 85%.

The charting of foam flows identifies patterns of foam, gas and water. The effect of surfactants is such that a foam phase, which is a mixture of gas and water, is always present.

In a typical experiment the liquid flow rate is fixed and the gas flow rate is varied. Fig. 9 shows several pressure profiles for various quality values (gauge pressure as a function of manometer

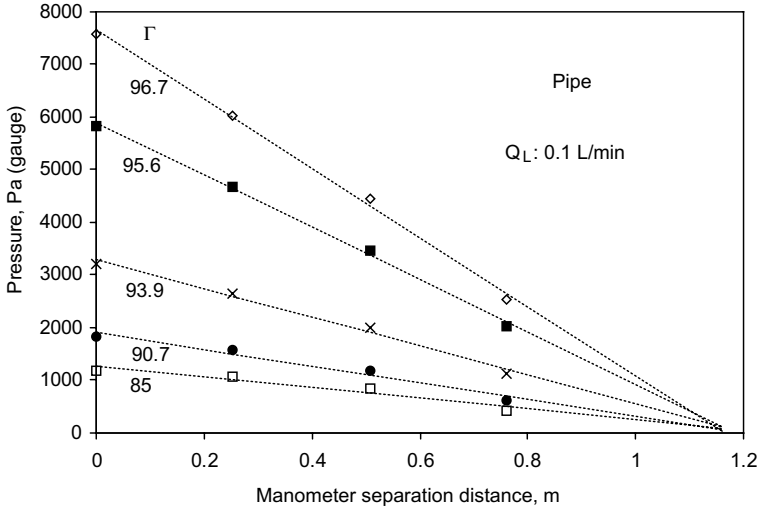

Fig. 9. Pressure variation with manometer separation distance as quality (Γ) increases from 85% to 96.7%. Liquid flow rate is constant, 0.1 l/min. Dashed lines correspond to linear fits to experimental data.

position) obtained at the pipe and a constant liquid flow rate of 0.1 l/min. Dashed lines shown in Fig. 9 correspond to calculated values from slope and intercept obtained by means of a linear regression. It can be observed that pressure varies linearly along the pipe and, as quality increases (or gas flow rate), pressure increases.

A linear pressure profile is a clear indication of a fully developed flow pattern and that there is not a significant expansion of foam bubbles along the pipe, which would imply on the one hand a flow acceleration and on the other an increase of bubble size and quality along the pipe. This was expected since pressure drop was never higher than 0.2 bar.

The linearity of the pressure gradient shows that, with only a small error, we may identify the pressure gradient $\mathrm{d}P/\mathrm{d}z$ with the pressure drop per unit length

$$\frac{\partial P}{\partial z} \cong \frac{\Delta P}{L}, \tag{2}$$

which is easier to measure. The pressure gradient as a function of foam quality for different liquid flow rates is shown for a channel (a) and a pipe (b) in Fig. 10. For a given liquid flow rate, pressure drop increases as gas flow rate (or quality) is increased. The trend is first linear and seems to be independent of liquid flow rate; when (Γ) is increased past 80% (dry foam) the pressure gradient increases very rapidly.

We found that increasing the gas flow rate reduced the bubble size when the quality was in the range of 95–97%; for larger values ($\Gamma > 97\%$), the bubble size increased. However, bubble size was much more affected by increasing liquid flow rate. This can be observed in Fig. 11 where two photographs are shown, the first (a) corresponds to a liquid flow rate of 0.02 l/min and a quality value of 96.6% and the second (b) to a liquid flow rate of 0.1 l/min and a quality value of 96.7%. An overall reduction of bubble size is apparent for the higher liquid flow rate. As liquid flow rate increases, it is necessary to squeeze a larger gas volume to maintain a constant quality and this is achieved by a reduction of bubble size. The increase of pressure due to higher flow could also be responsible for the bubble size reduction, but the pressure variations were too small to account for significant changes in bubble size.

In Fig. 12 we have plotted the pressure gradient against the superficial mixture velocity.

$$U_{\mathrm{M}} = U_{\mathrm{L}} + U_{\mathrm{G}} = \frac{Q_{\mathrm{L}} + Q_{\mathrm{G}}}{A}, \tag{3}$$

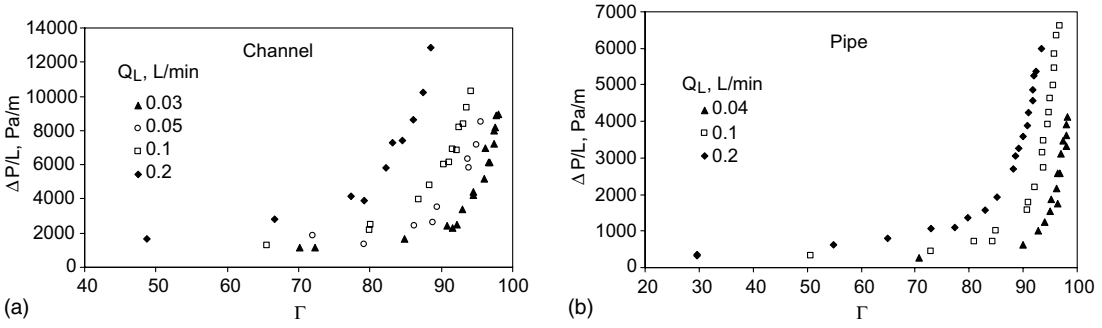

Fig. 10. Pressure gradient as a function of quality in (a) channel and (b) pipe; liquid flow rate is the parameter.

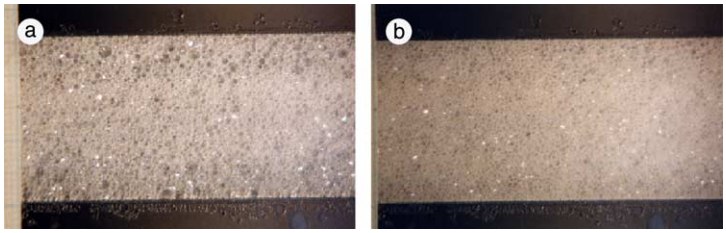

Fig. 11. Photographs of foam flowing in the channel for two different liquid flow rates and similar quality. (a) $Q_L = 0.02$ l/min, $\Gamma = 96.6\%$; (b) $Q_L = 0.1$ l/min, $\Gamma = 96.6\%$. A global reduction of bubble size can be observed for the higher liquid flow rate foam (photograph b).

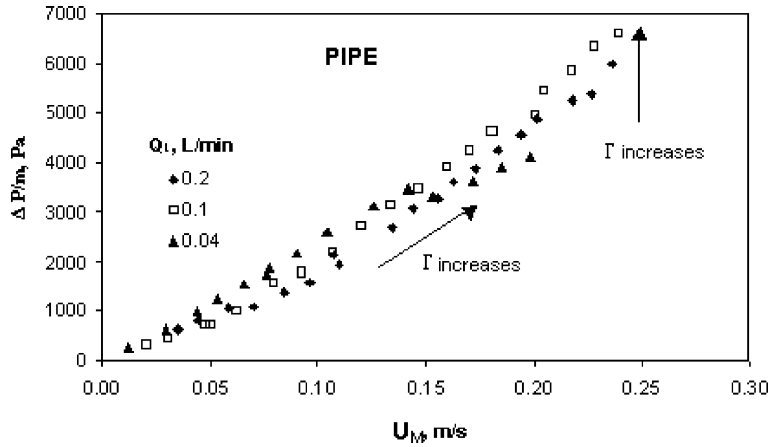

Fig. 12. Pressure gradient as a function of foam velocity and liquid flow rate in the pipe. Arrows point in the direction quality increases; i.e., quality increases as foam velocity and pressure gradient increase. The pressure gradient for $Q_L = 0.04$ l/min drops abruptly at about $U_M = 0.14$ m/s.

where A is the cross-sectional area of pipe and U_G and U_L are superficial velocities of the gas and liquid, respectively, for three different flow rates. The foam velocity is basically the same as the mixture velocity. The main point of interest is an apparent drop in the pressure gradient for the smallest value of liquid flow rate ($Q_L = 0.04$ l/min) at or near $U_M = 0.14$ m/s. This drop can be identified as a transition to slug flow which we have previously identified for foam quality above 97%.

Fig. 13 shows the pressure gradient vs foam velocity for the smallest liquid flow rate, $Q_L = 0.04$ l/min in the pipe and $Q_L = 0.03$ l/min in the channel. This plot identifies the abrupt drop in the pressure gradient with foam quality $\Gamma > 97\%$ where the transition to slug flow occurs.

Quality varies as shown by arrows in Fig. 12; for a constant liquid flow rate, the quality increases as U_M increases because more gas is being injected. Conversely, for a constant foam velocity the foam quality decreases as the liquid flow rate increases. The drop in the pressure gradient for $Q_L = 0.04$ l/min at about $U_M = 0.14$ m/s is severe; the pressure gradient which was greatest before the drop is the least after the drop.

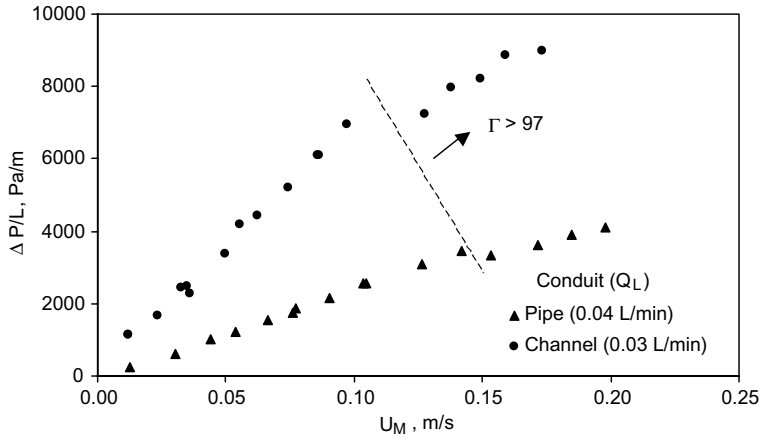

Fig. 13. Comparison of pressure gradient as a function of foam velocity for pipe and channel and a liquid flow rate of 0.04 l/min (pipe) and 0.03 l/min (channel). The dashed line indicates the transition to slug flow that occurs for $\Gamma > 97\%$.

5. Theory

An analysis of self-lubricated foam flow under ideal conditions will now be given. It is supposed that a rigid foam flows as a plug flow lubricated by water. The aim of the analysis is to predict the thickness of the water layer. It begins with the usual force balance between the pressure drop ΔP and wall shear stress τ_w

$$\Delta P A_c = \tau_w A_f, \tag{4}$$

where

$$A_f = L\ell_p. \tag{5}$$

L is the length of the conduit and ℓ_p is the length of its perimeter. Assuming now that the water layer is thin so that the velocity gradient $\partial v/\partial y$ in the water is given by

$$\frac{\partial v}{\partial y} \approx \frac{U_M}{\delta}, \tag{6}$$

where δ is the film thickness, we have

$$\tau_w = \mu_L \frac{U_M}{\delta}, \tag{7}$$

where μ_L is the water viscosity. Combining now (4)–(6), we find that

$$\delta = \frac{\ell_p \mu_L U_M}{A\left(-\frac{\Delta P}{L}\right)}. \tag{8}$$

For the pipe $\ell_p/A = 2/R_o$, where R_o is the pipe radius. For the channel $\ell_p/A = 2(d+H)/Hd$, where d is the depth and H is the height of the channel. ΔP and U_M are taken from the experiments.

5.1. Thickness of the lubrication layer

Values of δ computed from (8) are shown as a function of foam quality in Fig. 14. The thickness of the computed layer for uniform flow ($\Gamma > 80\%$) varies between 5 and 8 μm for the channel and 10 and 12 μm for the pipe. The small size of the layer is ex post facto consistent with the model assumptions.

In the range of quality comprised between approximately 77% and 97%, the lubricating layer tends to diminish as quality increases. This quality range corresponds to the conditions for which plug flow or nearly plug flow was obtained. Decrease of lubricating film thickness is consistent with decreasing of liquid content as foam dries. For $\Gamma < 77\%$ and $\Gamma > 97\%$, (8) does not hold very well given that flow is either stratified (dry foam on top of liquid layer), or slug flow. If we assume a value for δ (say $6 < \delta < 10$ μm), we may compute the foam velocity from the pressure gradient.

5.2. Friction factor vs. Reynolds number

Data on the pressure drop as a function of foam flow rate is plotted in dimensionless form in log–log variables as the friction factor

$$f_{\mathrm{m}} = \frac{\tau_{\mathrm{w}}}{\frac{1}{2}\rho_{\mathrm{L}} U_{\mathrm{M}}^2}, \quad \tau_{\mathrm{w}} = \frac{A\Delta P}{L\ell_{\mathrm{p}}} \tag{9}$$

as a function of Reynolds number

$$Re_{\mathrm{L}} = \frac{\rho_{\mathrm{L}} U_{\mathrm{M}} A}{\mu_{\mathrm{L}} \ell_{\mathrm{p}}} \tag{10}$$

where $A/\ell_{\mathrm{p}} = D_{\mathrm{h}}$ is the hydraulic diameter discussed under (5). These definitions are like those used for self-lubrication of bitumen froth (Joseph et al., 1999) in which the center line velocity

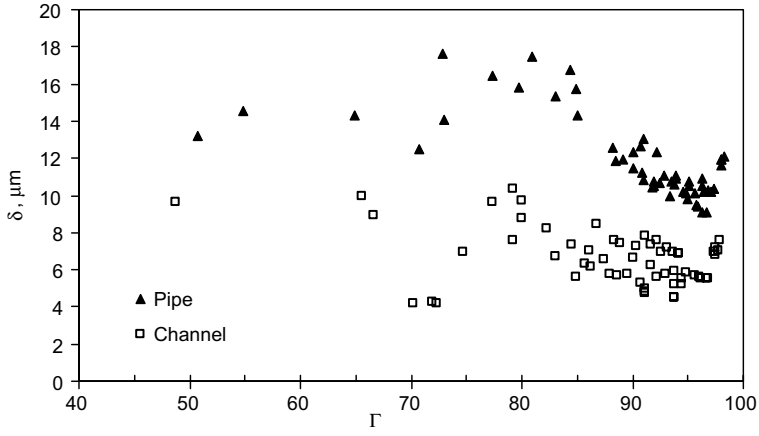

Fig. 14. Lubricating film thickness as a function of quality for pipe (triangles) and channel (squares). Data for each conduit correspond to different liquid flow rates but no distinction is made since no trend with the latter was found. For quality values larger than 80%, film thickness is about 5–8 μm for the channel and 10–12 μm for the pipe.

(core or foam velocity) is used together with the density and the viscosity of the lubricating layer (water) on the wall. The dimensionless plot is shown in Fig. 15. The data for our experiment in round pipes and channel as well as data obtained by Smieja (2000) clusters around a straight line corresponding to the power law

$$f_{\mathrm{M}} = \frac{3700}{Re_{\mathrm{L}}^{1.03}} \tag{11}$$

with an error measure $r^2 = 0.933$. The friction factor for round pipes is somewhat smaller than for channels, probably because the average lubricating layer thickness of 10–12 μm, is slightly larger than the average thickness of 5–8 μm in the channel. Eq. (11) should be compared with the well known formula

$$f = \frac{16}{Re} \tag{12}$$

for laminar flow of a single Newtonian liquid in a pipe. The exponent of 1.03 is only slightly larger than unity but 3700 is more than 200 times larger than 16. This huge increase in friction is probably due to the mechanism of self-lubrication which looks to the creation of a small lubrication layer by breaking foam at the wall.

An estimate of the size of this lubrication layer from the power law follows from replacing the exponent 1.03 with unity in (11) and the term $A\Delta P/L\ell_{\mathrm{p}}$ in (9) with the expression $\mu_{\mathrm{L}} U_{\mathrm{M}}/\delta$ from (8). This gives

$$\delta = \frac{2D_{\mathrm{h}}}{3700}. \tag{13}$$

For the 5/8 in. diameter pipe, we compute

$$\delta = 9\ \mu\mathrm{m}. \tag{14}$$

The high friction factor is then due to the fact that the size of the lubrication layer is very small.

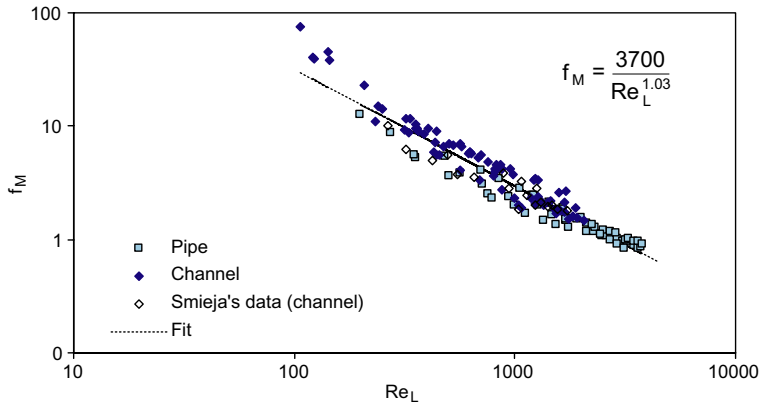

Fig. 15. Friction factor of foam as a function of Re_{L} for horizontal conduits. Data of Smieja (2000) obtained in a horizontal channel have been included.

We do not believe that the film thickness is really uniform as it is assumed in the ideal theory leading to (8). In fact, the film thickness is larger at the bottom due to drainage and the levitation of the foam due to gravity. The lubrication water is actually produced by foam which breaks under the action of the shear stress at the wall.

6. Conclusions

We did experiments on flow of aqueous foam in a horizontal channel and horizontal pipe. The flow rates of gas and liquid which determine foam quality were prescribed. Pressure gradients and foam flow rate were measured. Seven flow patterns were observed and correlated with foam quality and superficial velocity of the foam. The flow patterns are similar to those observed for gas–liquid flow with the caveat that three phases, water–gas–foam, rather two phases are involved. The lubricated flow is associated with uniform flow in the quality range $89\% \geqslant \Gamma \geqslant 97\%$.

Our main result is that aqueous foam will self-lubricate when it is easier to break the foam at the wall than to shear it internally. This mechanism leads to a lubricated laminar flow with a high friction associated with a small effective lubricating layer of water. The formation of lubrication layers depends on the strength of the bridges between the foam and the wall and possibly on wetting properties of the pipe wall.

Acknowledgements

This work was supported by the DOE, Engineering Division of the Department of Basic Energy Sciences; by the National Science Foundation under grants NSF/CTS-0076648 and NSF/CTS-0109029 (GOALI); by FONACIT-Venezuela under grant S1-2001001166 and by the School of Chemical Engineering of Los Andes University, Venezuela.

References

Bekkour, K., 1999. Evaluation of slip effects in the capillary flow of foams. Appl. Rheol. 9, 10–16.

Blondin, E., Doubliez, L., 2002. Particle imaging velocimetry of a wet aqueous foam with an underlying liquid film. Exp. Fluids 32, 294–301.

Calvert, J.R., 1990. Pressure drop for foam flow through pipes. Int. J. Heat Fluid Flow 11, 236–241.

Calvert, J.R., Nezhati, K., 1986. A rheological model for a liquid–gas foam. Int. J. Heat Fluid Flow 7, 164–168.

Deshpande, N.S., Barigou, M., 2000. The flow of gas–liquid foams in vertical pipes. Chem. Eng. Sci. 55, 4297–4309.

Deshpande, N.S., Barigou, M., 2001a. Foam flow phenomena in sudden expansions and contractions. Int. J. Multiphase Flow 27, 1463–1477.

Deshpande, N.S., Barigou, M., 2001b. The flow of gas–liquid foams through pipe fittings. Int. J. Heat Fluid Flow 22, 94–101.

Enzerdofer, C., Harris, R.A., Valkó, P., Economides, M.J., 1995. Pipe viscometry of foams. J. Rheol. 39, 345–358.

Gardiner, B.S., Dlugogorski, B.Z., Jameson, G.J., 1998. Rheology of fire-fighting foams. Fire Safety J. 31, 61–75.

Heller, J.P., Kuntamukkula, M.S., 1987. Critical review of the foam rheology literature. Ind. Eng. Chem. Res. 26, 318–325.

Jastrzebski, Z.D., 1967. Entrance effects and wall effects in an extrusion rheometer during flow of concentrated suspensions. Ind. Eng. Chem. Fund. 6, 445–454.

Joseph, D.D., Bai, R., Mata, C., Sury, K., Grant, C., 1999. Self-lubricated transport of bitumen froth. J. Fluid Mech. 386, 127–148.

Khan, S.A., 1987. Foam rheology: relation between extensional and shear deformations in high gas fraction foams. Rheol. Acta 26, 78–84.

Khan, S.A., Armstrong, R.C., 1986. Rheology of foams: I. Theory for dry foams. J. Non-Newtonian Fluid Mech. 22, 1–22.

Khan, S.A., Schnepper, C.A., Armstrong, R.C., 1988. Foam rheology: III. Measurement of shear flow properties. J. Rheol. 32, 69–92.

Mooney, M., 1931. Explicit formulas for slip and fluidity. J. Rheol. 2, 210–222.

Rojas, Y., Kakadjian, S., Aponte, A., Márquez, R., Sánchez, G., 2001. Stability and rheological behavior of aqueous foams for underbalanced drilling. In: SPE International Symposium on Oilfield Chemistry, paper SPE 64999, Houston, 13–16 February 2001.

Smieja, T., 2000. Some experiments on the flow dynamics of foams and particle laden flows. MS dissertation, University of Minnesota, Minneapolis.

Tisnè, P., Aloui, F., Doubliez, L., 2003. Analysis of wall shear stress in wet foam flows using the electrochemical method. Int. J. Multiphase Flow 29, 841–854.

Valkó, P., Economides, M.J., 1992. Volume equalized constitutive equations for foamed polymer solutions. J. Rheol. 36, 1033–1055.